Supporting Information

Dual-Accepting-Unit Design of Donor Material for All-Small-Molecule Organic Solar Cells with Efficiency Approaching 11%

Yong Huo, Xiao-Ting Gong, Tsz-Ki Lau, Tong Xiao, Cenqi Yan, Xinhui Lu, Guanghao Lu*, Xiaowei Zhan* and Hao-Li Zhang*

Contents

1 Materials

Unless stated otherwise, all the solvents and chemical reagents were obtained commercially and used without further purification. All reactions dealing with air- or moisture-sensitive compounds were carried out using standard Schlenk techniques. The compound 1[1] and compound 5[2] were synthesized according to the literatures.

Scheme S1. The synthetic routes for SBDT-BDD.

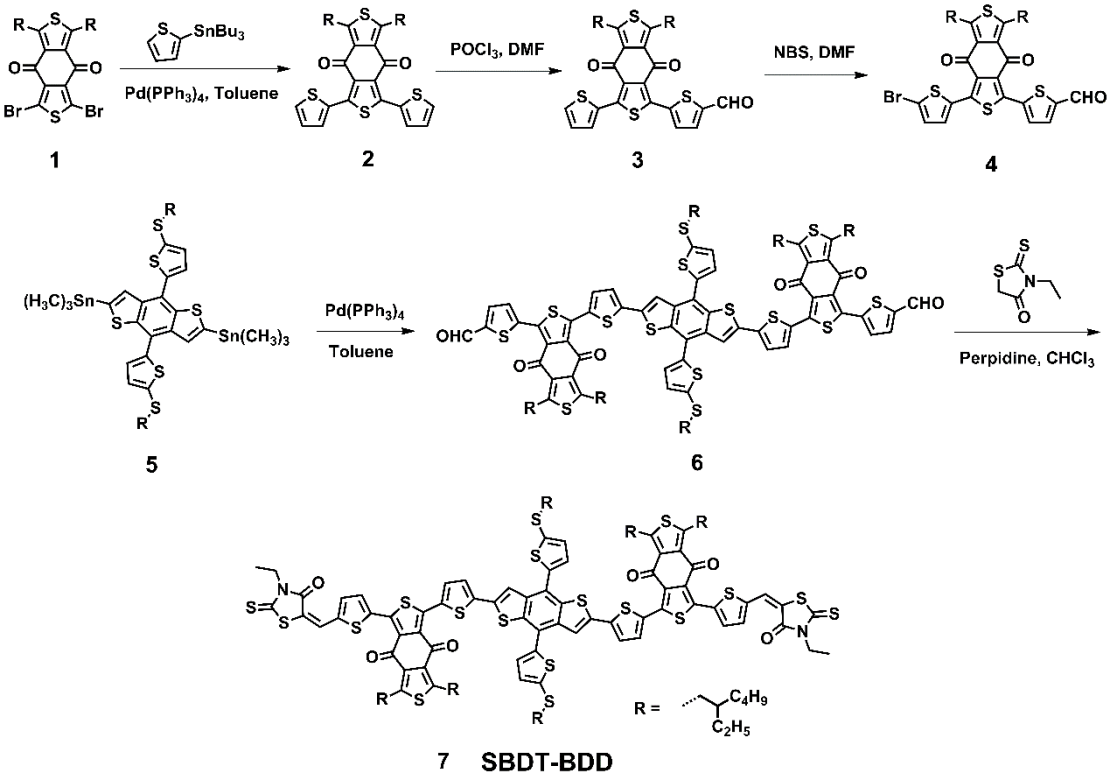

Compound 2 (1,3-bis(2-ethylhexyl)-5,7-di(thiophen-2-yl)benzo[1,2-c:4,5-c'] dithiophene-4,8-dione). Under the protection of argon, $Pd(PPh_3)_4$ (40 mg) was added to a solution of compound 1 (603 mg, 1 mmol) and thimethyl(thiophen-2-yl)stannane (1119 mg, 3 mmol) in 20 mL of toluene. The mixture was refluxed for 12 h. After the removal of the solvent at a reduced pressure, the residue was purified by columnchromatography on a silica gel column with petroleum ether/dichloromethane (5:1 by volume) to give a yellow solid (536 mg, 88 %).

^{1}H NMR (400 MHz, $CDCl_3$): δ7.74 (d, 2H), 7.50 (d, 2H), 7.11 (t, 2H), 3.32(m, 4H), 1.76 (m, 2H), 1.42-1.26 (m, 16H), 0.94−0.87 (m, 12H).

Compound 3 (5-(5,7-bis(2-ethylhexyl)-4,8-dioxo-3-(thiophen-2-yl)-4,8-dihydro benzo[1,2-c:4,5-c']dithiophen-1-yl)thiophene-2-carbaldehyde). In a 50 mL flask, 0.15 mL $POCl_3$ was added slowly to 0.2 mL of dimethylformamide (DMF) at 0 °C and stirred at this temperature for 30 min. Then compound 2 (609 mg, 1 mmol) in 1, 2-dichloroethane (20 mL) solution was added dropwise at 0 °C. The mixture was stirred at 85 °C for 12 h and then poured into water, neutralized with sodium bicarbonate, extracted with CH_2Cl_2, and dried with anhydrous $MgSO_4$. The solvent was removed via rotary evaporation, and the residue was purified by column chromatography on silica gel with petroleum ether/dichloromethane (1:1 by volume) to give a colorless oil (382 mg, yield = 60 %). ^{1}H NMR (400 MHz, $CDCl_3$): δ9.96 (d, 1H), 7.74 (d, 2H), 7.62 (m, 1H), 7.12 (m, 2H), 3.36-3.28 (t, 4H), 1.76 (s, 2H), 1.41-1.26 (m, 16H), 0.94-0.88 (m, 12H).

Compound 4 (5-(3-(5-bromothiophen-2-yl)-5,7-bis(2-ethylhexyl)-4,8-dioxo-4,8-dihydrobenzo[1,2-c:4,5-c']dithiophen-1-yl)thiophene-2-carbaldehyde). Compound 3 (637 mg, 1 mmol) was added into DMF (20 mL). After the solid dissolved completely, N-bromosuccinimide (NBS) (256 mg, 2 mmol) was added in several times. The reaction mixture was stirred at room temperature for 8 h, water was added into the mixture, the mixture was extracted with CH_2Cl_2, and the organic layer was washed with brine and dried over anhydrous sodium sulfate. The solvent was removed at a reduced pressure; the residue was purified by column chromatography on silica gel with petroleum ether/dichloromethane (1:1 by volume) to give a red solid (680 mg, yield = 95%).^{1}H NMR (400 MHz, $CDCl_3$): δ9.88 (s, 1H), 7.61 (s, 1H), 7.39 (s, 1H), 7.24 (s, 1H), 7.00 (s, 1H), 3.39-3.26 (m, 4H), 1.76 (s, 2H), 1.42-1.26 (m, 16H), 0.96-0.87 (m, 12H).

Compound 6 (5,5'-(3,3'-(5,5'-(4,8-bis(5-((2-ethylhexyl)thio)thiophen-2-yl)benzo [1,2-b:4,5-b']dithiophene-2,6-diyl)bis(thiophene-5,2-diyl))bis(5,7-bis(2-ethylhexyl) -4,8-dioxo-4,8-dihydrobenzo[1,2-c:4,5-c']dithiophene-3,1-diyl))bis(thiophene-2-carbaldehyde)). A solution of compound 5 (97 mg, 0.1 mmol) and compound 4 (150 mg，0.21 mmol) in 20 mL dry toluene was degassed twice with argon following the addition of $Pd(PPh_3)_4$ (60 mg, 0.05 mmol). After being stirred and refluxed for 24 h at 110 °C with the protection of argon, the reaction mixture was poured into water (100 mL) and extracted with $CHCl_3$. The organic layer was washed with water twice and dried over anhydrous Na_2SO_4 for 1 h. After removal of solvent, the crude product was purified by silica gel using petroleum ether/dichloromethane (1:1 by volume) as eluant to afford a black solid (124 mg, yield = 66%).^{1}H NMR (400 MHz, $CDCl_3$): δ9.91 (s, 2H), 7.70 (d, 2H), 7.66 (t, 4H), 7.63 (s, 2H), 7.34 (d, 2H), 7.11 (d, 2H), 6.96 (d, 2H), 3.26-3.23 (m, 8H), 2.94-2.92 (m, 4H), 1.78-1.72 (m, 6H), 1.40-1.26 (m, 48H), 1.03-0.87 (m, 36H). MS (MALDI-TOF): m/z 1911.7 (M^+). Anal. calcd for $C_{104}H_{118}O_6S_{12}$: C, 65.30; H, 6.22. Found: C, 65.42; H, 6.27.

Compound 7 (SBDT-BDD) ((E)-7,7'-(5,5'-(4,8-bis(5-((2-ethylhexyl)thio)thiophen -2-yl)benzo[1,2-b:4,5-b']dithiophene-2,6-diyl)bis(thiophene-5,2-diyl))bis(5-(5-((E)-(3-ethyl-4-oxo-2-thioxothiazolidin-5-ylidene)methyl)thiophen-2-yl)-1,3-bis(2-ethylhexyl)benzo [1,2-c:4,5-c']dithiophene-4,8-dione)). Compound 6 (192 mg, 0.10 mmol) and 3-ethylrhodanine (161 mg, 1 mmol) were dissolved in 30 mL dry $CHCl_3$ solution under the protection of argon, and then three drops of piperidine were added to the mixture. After being stirred and refluxed for 12 h at 60 °C, the mixture was extracted with $CHCl_3$, and the organic layer was washed with water and dried over anhydrous Na_2SO_4 for 1 h. After removal of solvent, the crude product was purified by silica gel using chloroform as eluant to afford a black solid (160 mg, yield = 67%). ^{1}H NMR (400 MHz, $CDCl_3$): δ 7.62 (m, 4H), 7.46 (m, 4H), 7.29 (d, 2H), 7.14 (s, 2H), 6.93 (d, 4H), 4.17-4.11 (m, 4H), 3.31-3.26 (m, 8H), 2.94-2.92 (m, 4H), 1.77-

1.21 (m, 50H), 1.06-0.87 (m, 36H). MS (MALDI-TOF): m/z 2197.6 (M^+). Anal. calcd for $C_{114}H_{128}N_2O_6S_{18}$: C, 62.25; H, 5.87. Found: C, 62.36; H, 5.92.

2 Characterization

The ^1H NMR spectra were measured using a Bruker AVANCE 400 MHz spectrometer. Mass spectra were measured using Bruker Daltonics Biflex III MALDI-TOF Analyzer in the MALDI mode. UV-vis absorption spectra in solution (chloroform) and thin film (on a quartz substrate) used Jasco V-570 spectrophotometer. Elemental analysis was carried out using a Flash EA 1112 elemental analyzer. Electrochemical measurements were carried out under nitrogen in a deoxygenated solution of tetra-*n*-butylammoniumhexafluorophosphate (0.1 M) in acetonitrile using a potential scan rate of 100 mV s^{-1} employing a computer-controlled Zahner IM6e electrochemical workstation. All measurements were carried out at room temperature with a conventional three electrode configuration consisting of a platinum working electrode, a platinum wire auxiliary electrode, and a nonaqueous Ag/AgNO3 reference electrode. Dichloromethane was distilled from calcium hydride under dry nitrogen immediately prior to use. The potentials were referenced to a ferrocenium/ferrocene ($FeCp_2^{+/0}$) couple using ferrocene as an external standard. Thermogravimetric analysis (TGA) measurements were performed using a Shimadzu thermogravimetric analyzer (Model DTG-60) under flowing nitrogen gas at a heating rate of 10 °C min^{-1}. The nanoscale morphology of the blended films was observed using a Multimode 8 atomic force microscope (Bruker) in the tapping mode. GIWAXS and GISAXS measurements were carried out by an in-house device Xeuss2.0 manufactured by Xenocs. The X-ray source is Cu and the wavelength is 1.54Å. The incidence angle is 0.2°.

Fabrication and characterization of the SM-OSCs and NFASM-OSCs

The small molecule solar cell devices were fabricated and characterized in a N2-filled glovebox. The device structure was ITO/PEDOT:PSS/small molecule:$PC_{71}BM$/ ZrAcac/Al for ASM-OSCs. Patterned ITO glass (sheet resistance = 15 Ω $□^{-1}$) was precleaned in an ultrasonic

bath with acetone and isopropanol, and treated in an ultraviolet–ozone chamber (Jelight Company, USA) for 20 min. PEDOT:PSS layer (*ca.* 30 nm) was spin-coated at 4000 rpm onto the ITO glass, and then baked at 150 °C for 15 min. Then donor:acceptor mixture solutions (15 mg mL^{-1} in total for binary devices and 17 mg mL^{-1} in total for ternary devices) in chloroform were spin-coated (*ca*. 100 nm). After spin-coating, the active layers were optimized with CS_2 solvent vapor annealing treatment. Then ethanol solution of ZrAcac at a concentration of 1.0 mg mL^{-1} was spin-coated at 3000 rpm (*ca*. 5 nm) onto the active layer. At last, Al electrode (*ca*. 80 nm) was slowly evaporated onto the surface of the photoactive layer under vacuum (*ca*. 10^{-5} Pa). The active area of the device was *ca.* 4 mm^2. The *J-V* curve was measured using a computer-controlled B2912A Precision Source/Measure Unit (Agilent Technologies). An XES-70S1 (SAN-EI Electric Co., Ltd.) solar simulator (AAA grade, 70 × 70 mm^2 photobeam size) coupled with AM 1.5 G solar spectrum filters was used as the light source, and the optical power at the sample was 100 mW cm^{-2}. A 2 × 2 cm^2 monocrystalline silicon reference cell (SRC–1000-TC-QZ) was purchased from VLSI Standards Inc. The EQE spectrum was measured using Solar Cell Spectral Response Measurement System QE-R3011 (Enlitech Co., Ltd.). The thickness of organic layer was measured on DektakXT (Bruker).

Mobility measurements

Hole-only or electron-only devices were fabricated using the architectures of ITO/PEDOT: PSS/ active layer/Au for holes and glass/Al/ active layer /Al for electrons. For hole-only devices, the pre-cleaned ITO glass was spin-coated with PEDOT: PSS (*ca*. 35 nm), then active layers were spin-coated, then Au (*ca*. 30 nm) was evaporated under vacuum (*ca*. 10^{-5} Pa) at a low speed (1 Å/5 s) to avoid the penetration of Au atoms into the active layers. For electron-only devices, Al (*ca*. 80 nm) was evaporated onto pre-cleaned glass under vacuum (*ca*. 10^{-5} Pa), active layers was spin-coated, and then Al (*ca.* 50 nm) was evaporated under vacuum (*ca*. 10^{-5} Pa). The mobility was extracted by fitting the current density–voltage curves using space charge limited current (SCLC). The equation is as follows.

$J = (9/8)\mu\varepsilon_r\varepsilon_0 V^2 \exp(0.89(V/E_0 L)^{0.5})/L^3$

where J is current density, μ is hole or electron mobility, ε_r is relative dielectric constant, ε_0 is permittivity of free space, $V = V_{appl} - V_{bi}$, E_0 is characteristic field, L is the thickness of organic layer. The J–V curves of the devices are plotted as $\ln[Jd^3/(V_{appl}-V_{bi})^2]$ versus $[(V_{appl}-V_{bi})/d]^{0.5}$.

3 Cyclic voltammograms of SBDT-BDD

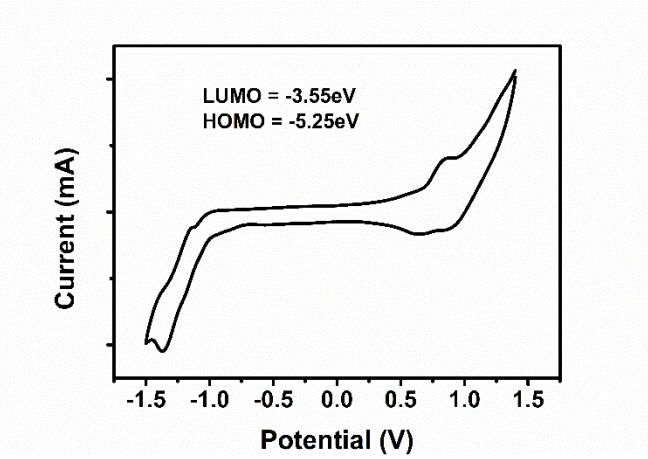

Figure S1 Cyclic Voltammograms of SBDT-BDD in dichloromethane solution.

Table S1. Optical and electrochemical data of SBDT-BDD.

Small molecule	$\lambda_{max,sol}$ (nm)	ε_{sol} ($M^{-1}cm^{-1}$)	$\lambda_{max,film}$ (nm)	ε_{film} (cm^{-1})	E_g^{opt} (eV)	IP[a] (eV)	EA[a] (eV)	E_g[a] (eV)
SBDT-BDD	521	8.5×10^4	590,627	4.5×10^4	1.77	5.25	3.55	1.70

[a] from Cyclic Voltammograms test, IP is ionization potential, EA is electron affinitie.

4 TGA test of SBDT-BDD

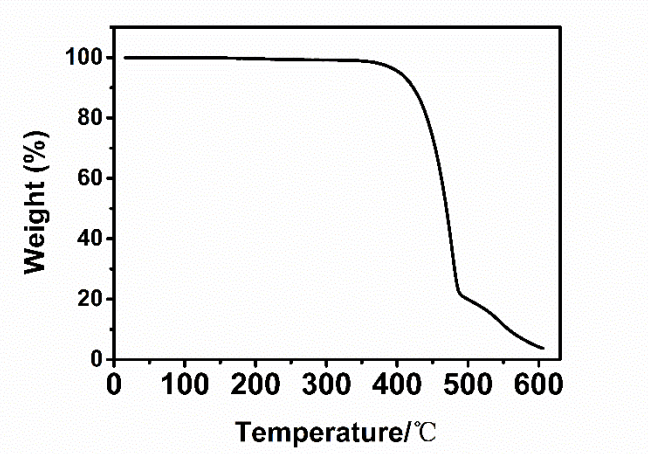

Figure S2 TGA plot of SBDT-BDD.

5 Hole mobilities of SBDT-BDD

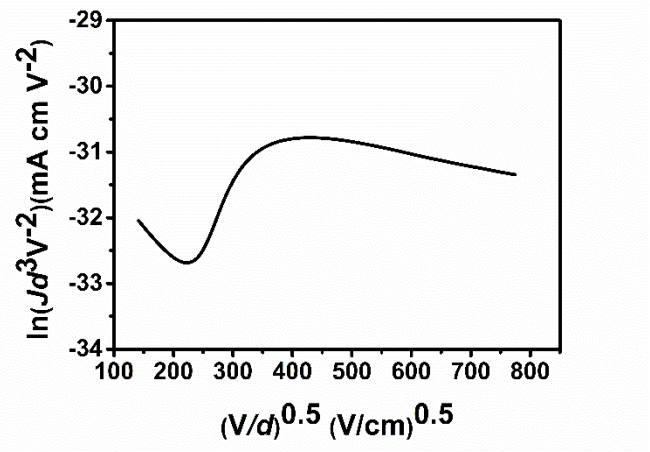

Figure S3 Hole mobilities of SBDT-BDD.

6 Device optimization for binary and ternary OSCs

Table S2. Binary device performance with different SBDT-BDD:IDIC ratios.

D:A	V_{OC} (V)	J_{SC} (mA cm^{-2})	FF (%)	PCE (%)
1:1.5	0.97	9.29	40.3	3.6
1:1	0.98	11.48	42.7	4.8
1.5:1	0.99	9.03	45.2	4.1

Table S3. Binary device performance with different time for CS_2 SVA treatment.

Time（s）	V_{OC} (V)	J_{SC} (mA cm^{-2})	FF (%)	PCE (%)
0	0.98	11.48	42.7	4.8
30	0.98	12.56	52.2	6.5
45	0.97	15.15	62.5	9.2
60	0.97	14.29	54.8	7.6

Table S4. Ternary device performance with different SBDT-BDD:IDIC:$PC_{71}BM$ ratios.

SM/IDIC/$PC_{71}BM$	V_{OC} (V)	J_{SC} (mA cm^{-2})	FF (%)	PCE^{c} (%)	J_{SC}^{cal} (mA cm^{-2})
1:1:0 (0%)	0.98	11.48	42.7	4.8	11.53
1:0.75:0.25 (25%)	0.98	10.93	42.1	4.5	10.66
1:0.5:0.5 (50%)	0.98	12.89	33.0	4.2	12.94
1:0.25:0.75 (75%)	0.99	11.63	35.5	4.1	11.76
1:0:1 (100%)	1.00	9.86	47.9	4.7	9.98

Table S5. Ternary device performance with CS_2 SVA treatment.

SM/IDIC/$PC_{71}BM$	V_{OC} (V)	J_{SC} (mA cm^{-2})	FF (%)	PCE[c] (%)	J_{SC}^{cal} (mA cm^{-2})
1:1:0 (0%)	0.97	15.15	62.5	9.2	14.75
1:0.75:0.25 (25%)	0.97	13.86	64.3	8.8	13.36
1:0.5:0.5 (50%)	0.97	16.21	69.3	10.9	15.91
1:0.25:0.75 (75%)	0.98	15.07	64.6	9.5	14.64
1:0:1 (100%)	0.99	12.28	66.3	8.1	11.98

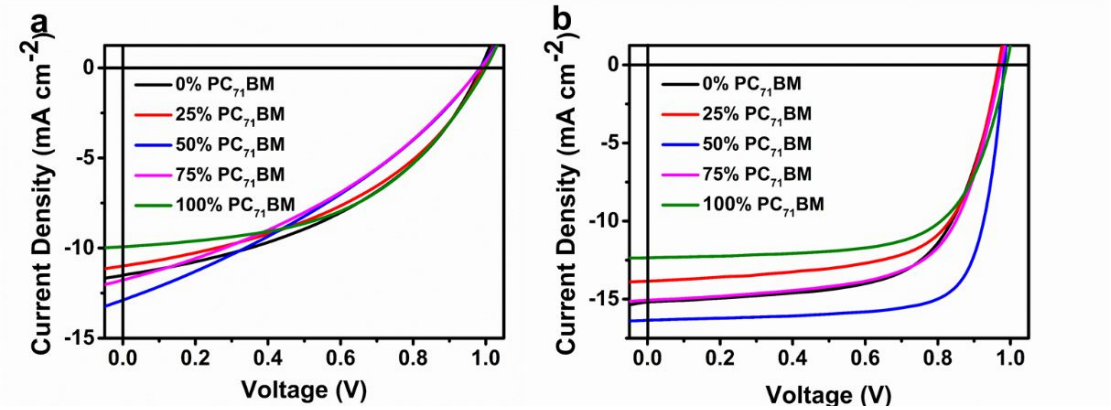

Figure S4 *J-V* characteristics of (a) as-cast and (b) SVA treatment ternary OSCs.

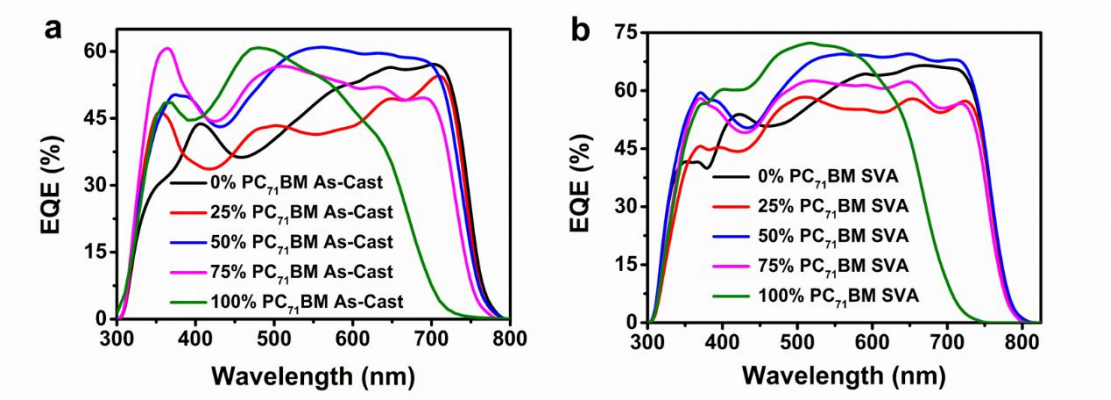

Figure S5 EQE curves of (a) as-cast and (b) SVA treatment ternary OSCs.

7 Binary and ternary film absorption spectra

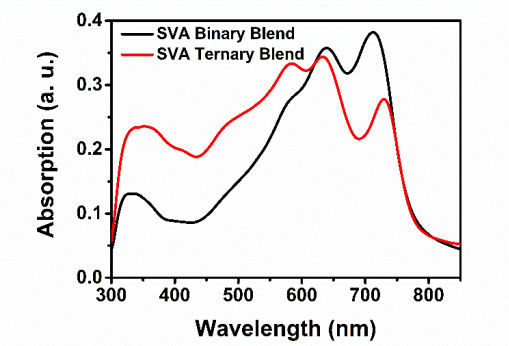

Figure S6 The UV-vis absorption spectra of binary and ternary film with SVA treatment.

8 Charge recombination

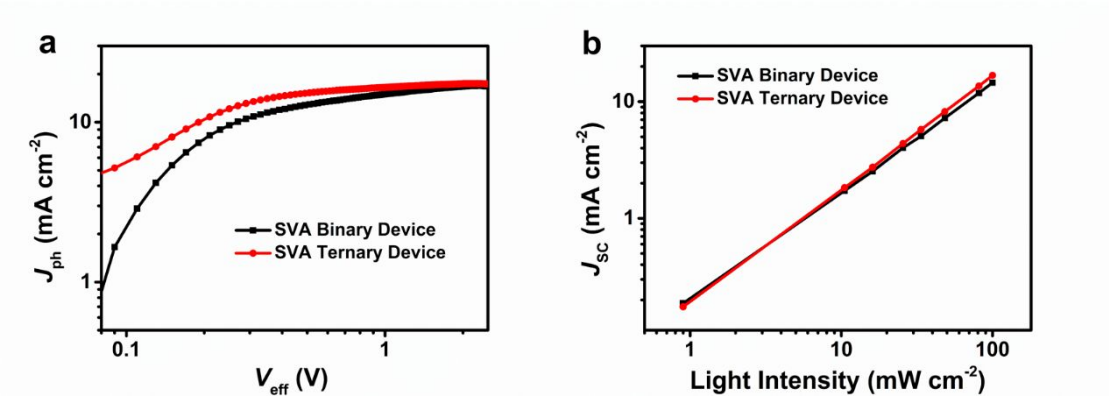

Figure S7 (a) J_{ph} versus V_{eff} characteristics and (b) J_{SC} versus light intensity for the best binary and ternary devices.

9 AFM images of binary and ternary films

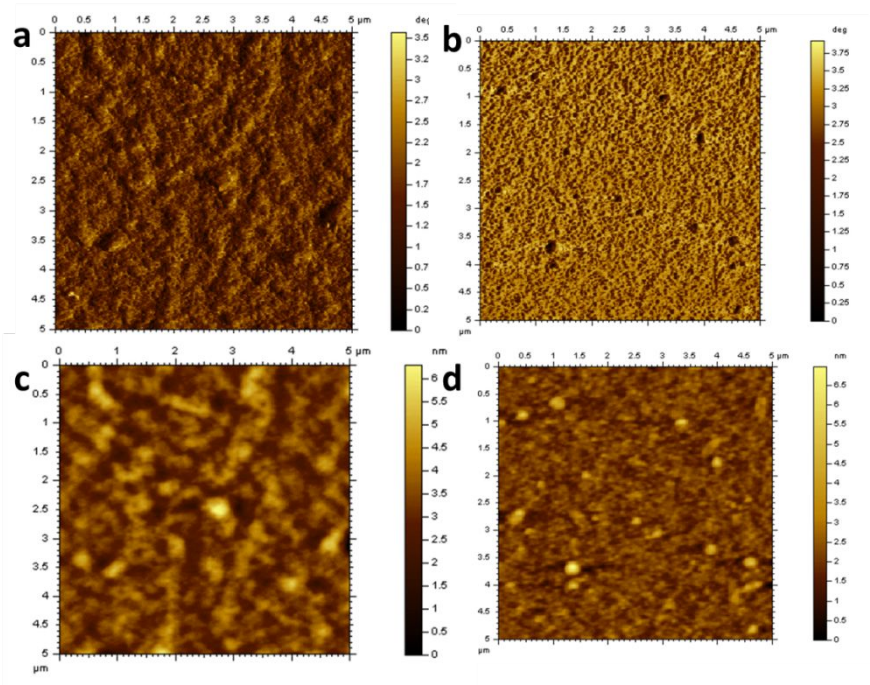

Figure S8 AFM phase images for (a) the best binary blend and (b) the best ternary blend, the corresponding height images for (c) the best binary blend and (d) the best ternary blend.

10 GIWAXS images for pure films

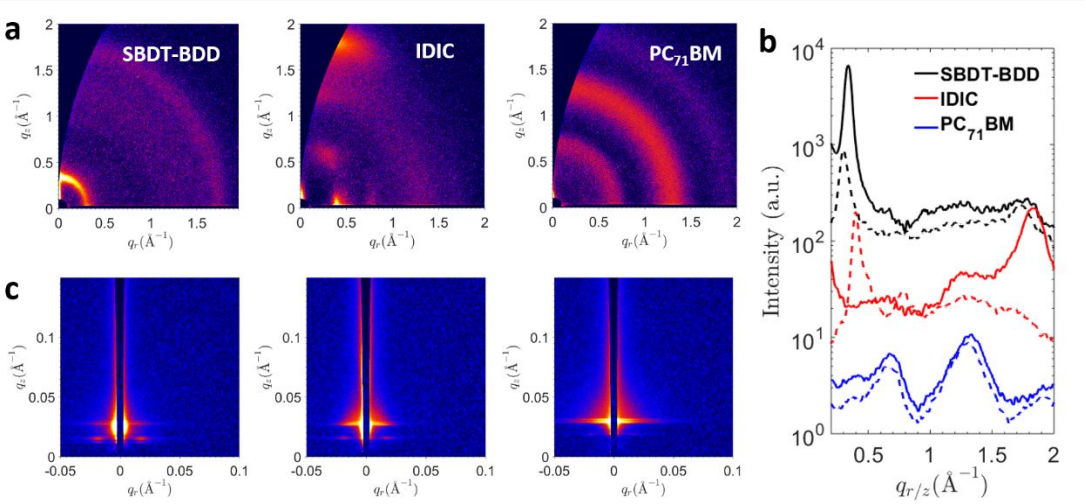

Figure S9 (a) The GIWAXS patterns of SVA pure films and (b) The corresponding intensity profiles along the in-plane (dashed line) and out-of-plane (solid line) directions. (c) The GISAXS patterns of SVA blend films.

11 Hole and electron mobilities tests of binary and ternary OSCs

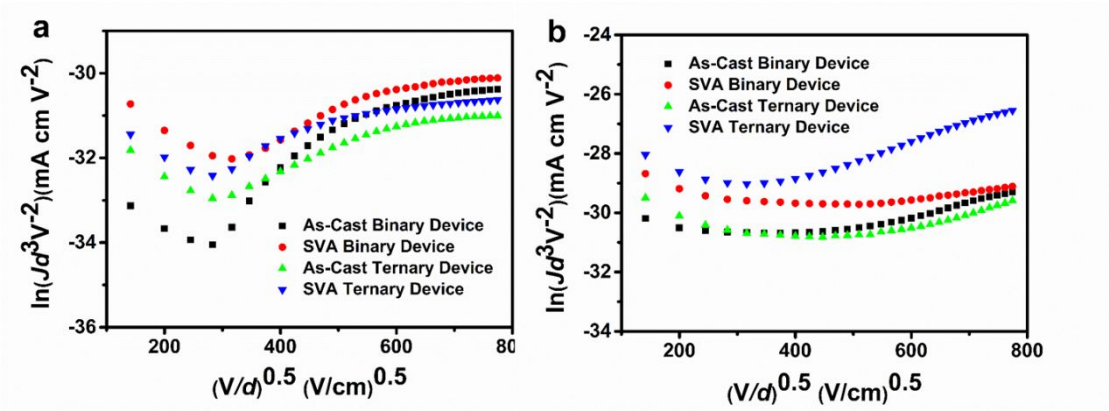

Figure S10 *J*-V characteristics in the dark for a) hole-only and b) electron-only devices based on best binary and ternary devices.

Table S6. The mobilities of best binary and ternary devices.

Device	μ_h/cm^2 V^{-1} s^{-1}	μ_e/cm^2 V^{-1} s^{-1}	μ_h/μ_e
Binary Device[a]	7.8×10^{-5}	2.1×10^{-5}	3.7
Binary Device[b]	1.3×10^{-4}	0.8×10^{-4}	1.6
Ternary Device[a]	9.8×10^{-5}	1.8×10^{-5}	5.4
Ternary Device[b]	2.2×10^{-4}	1.4×10^{-4}	1.5

[a] as-cast;[b] with CS_2 SVA 45s.

12 Simulated contours of energy dissipation *Q* and exciton generation rate *G* profiles

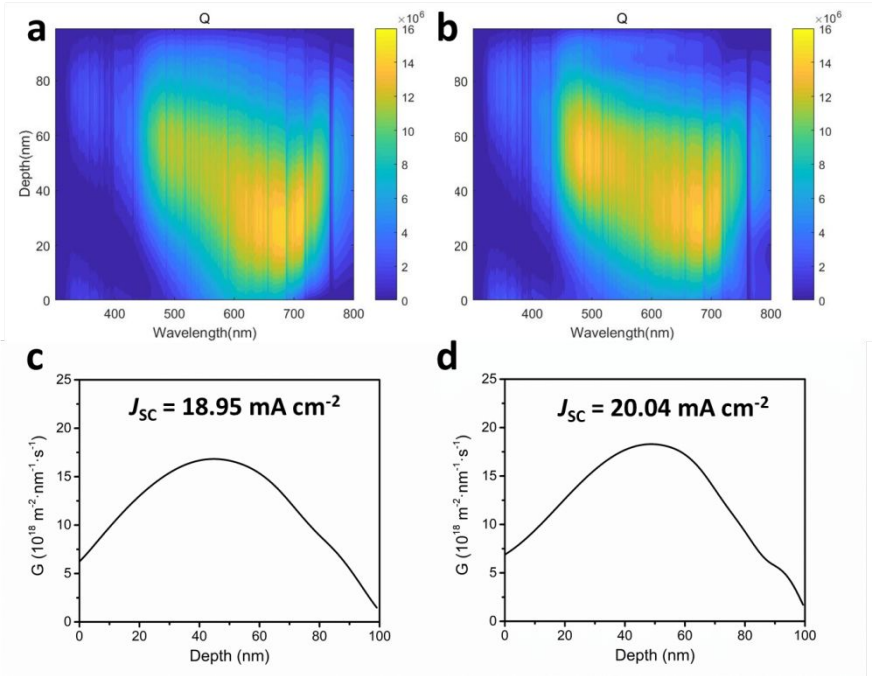

Figure S11 (a and b) Simulated contours of energy dissipation *Q* (unit, μWcm^{-3} nm^{-1} at its position and wavelength) and (c and d) exciton generation rate *G* profiles for as-cast binary and ternary devices.

13 References

1. D. Qian, L. Ye, M. Zhang, Y. Liang, L. Li, Y. Huang, X. Guo, S. Zhang, Z. a. Tan, J. Hou, Design, Application, and Morphology Study of a New Photovoltaic Polymer with Strong Aggregation in Solution State. *Macromolecules* **2012**, *45*, 9611-9617.
2. C. Cui, W. -Y Wong, Y. Li, Improvement of open-circuit voltage and photovoltaic properties of 2D-conjugated polymers by alkylthio substitution. Energy Environ. Sci. 2014, 7, 2276-2284.